Mechanism and rates of conformational transitions in heterogeneous polymers

Eugene Helfand

Bell Laboratories, Murray Hill, New Jersey 07974

Jeffrey Skolnick

Department of Chemistry, Louisiana State University, Baton Rouge, Louisiana 70803
(Received 11 June 1982; accepted 9 August 1982)

A general expression is presented for the rate of a *trans* to *gauche* conformational transition of a bond in a polymer backbone. The polymer is composed of nonidentical atoms, i.e., centers of differing friction constants and masses. The rate is obtained from a multidimensional extension of Kramers' steady state solution to the Fokker–Planck equation for flux over a reaction barrier of a system in a frictional medium. Langer's formulation is used. Results are appropriate for all but extremely small friction, with simplification occurring in the high friction limit. One also determines the reaction coordinate, an examination of which gives insight into the kinetic mechanism. Explicit results are obtained for six and 32 vertex chains, and the influence of chain conformation and relative friction constants are discussed.

I. INTRODUCTION

In a recent paper[1] we developed a theory of conformational transitions (*trans* $\rightleftharpoons$ *gauche*) for a chain molecule of identical units dissolved in a highly viscous solvent, i.e., in the high friction limit. Here, the theory of conformational transitions will be generalized to polymers containing nonidentical vertices; in particular, the mass and friction constant of every vertex will be allowed to be different. The goal is to determine, via a steady state solution to the Fokker–Planck equation, the rate of conformational transition k for a bond in a heterogeneous chain molecule. This rate is to be applicable from the high to low friction limit (but not so low as to make thermalization the limiting process). It will be seen that the presence of nonidentical vertex friction constants exerts an important influence on the nature of the reaction coordinate and thereby on the calculated rate of conformational transitions.

Of late, a considerable number of workers have focused on problems in polymer dynamics.[1–12] Since Ref. 1 has presented a fairly lengthy discussion of the relevant literature, we content ourselves here with a brief review of some of the salient points.

A fundamental quandary would seem to be as follows. Consider one bond in a chain and the attached polymers, the tails. Let the bond undergo a conformational transition. If there is no accompanying transition of any bonds of the tails, then the tails' positions in space after the transition differ markedly from the initial positions; i.e., they undergo a large rotational displacement. It has been assumed in the past that this prevented single transitions and that only special cooperative transitions of groups of bonds take place for which the initial and final position of the tails do not differ (crankshafts[13] or three-bond motions[14]).

Conformational transitions of bonds in polymer molecules have been studied by a variety of experimental methods.[9–12] These techniques provide a relaxation rate for local, i.e., molecular weight independent, reorientation processes believed to be related to conformational transitions. The Arrhenius plot of the temperature dependence of the relaxation rate gives an estimate of its activation energy $E^\dagger$. If $E^\dagger$ is approximately equal to the barrier height associated with conformational transitions about a single bond E^* then the single conformational transition event becomes plausible. On the other hand, if $E^\dagger$ is equal to $2E^*$ or to the *cis* barrier energy, a crankshaft or three-bond local motion may be implied.[13,14] Almost invariably, $E^\dagger$ is found experimentally to be quite close to E^*. This observation, together with similar results obtained in Brownian dynamics simulations,[6,7] lends credence to the viewpoint that conformational transitions need not proceed by the highly cooperative crankshaft modes, and may involve single rotational angle transitions.

While it may at first appear surprising that the elemental local motions in polymers can take place by single conformational transitions, further consideration reveals how this can be the case. As Keck[15] and Bennett[16] have observed, calculation of a transition rate requires knowledge of the distribution of states centered around the reaction barrier. It is precisely the character of the motion in the vicinity of the barrier that determines the kinetics of single conformational transitions. Therefore, the initial and final states of remote portions of the tails attached to the transforming bond are not of central importance. These observations on the nature of conformational transitions have been incorporated into the work of Skolnick and Helfand.[1]

Both the present treatment and Ref. 1 assume that conformational transitions in polymers occur through single independent transition events only. Thus, while the theory revealed good qualitative and fair quantitative agreement with rates of conformational transition obtained in recent Brownian dynamics simulations,[7] it cannot account for the observed short time behavior which reveals that some transition events are cooperative; i.e., an initial transition is accompanied for a short period afterward by an increased frequency of transitions of neighboring bonds. Nevertheless, the current approach should provide further qualitative insight

 021-9606/82/235714-11$02.10

into the factors involved in the mechanism of conformational transitions. Also the rates are semiquantitative to the extent that single transitions are the rate-determining process.

Our previous work[1,2] has revealed that the reaction coordinate in the vicinity of the bottleneck to the conformational transition (a saddle point on the potential surface in coordinate space) is a localized mode: the torsional distortion of the transforming bond couples into the motion of the neighboring vertices, but such motion decreases with increasing distance from the transforming bond.

For polymers composed of identical vertices, we have obtained a rate expression valid in the high friction regime.[1] The rate of transition depends on the torsional force constants, on the barrier height of the bond undergoing the transition, and on the vertex friction constant. The influence of the attached tails' conformation, potential, and orientation enters only in λ, the curvature of the reaction coordinate in the vicinity of the saddle point. The resulting rate formula is quite easy to apply and interpret. The treatment of heterogeneous polymers requires a more general approach to the barrier crossing, the problem to which we now turn.

Much attention has been devoted recently to the development of sophisticated theories for the rate of barrier crossing in one-dimensional systems. There is the kinetic theory approach of Skinner and Wolynes,[17] the stable states picture of Northrup and Hynes,[18] and Grote and Hynes,[19] and the trajectory analysis method of Montgomery, Chandler, and Berne.[20] However, we shall adopt the viewpoint that polymer conformational transitions in the intermediate friction regime are adequately described by the Fokker–Planck equation. We recognize, of course, that various models of the low to intermediate friction limit must be investigated, and we focus here on the one most akin to our previous work.

Blomberg has presented a detailed discussion of the one-dimensional Fokker–Planck equation for Brownian motion in a potential that is harmonic in the well and near the barrier to transitions.[21] Helfand[5] has simulated such a system on the computer. They find that the Kramers[22] solution to the Fokker–Planck equation is valid over a considerable range of the moderate damping regime. Thus, we feel the present approach affords a realistic possibility of adequately describing transition dynamics in the intermediate friction region.

The multidimensional version of the high friction limit of Kramers reaction rate theory[22] has been derived by Brinkman,[23] Landauer and Swanson,[24] Langer,[25,26] and others. Langer,[26] in a treatment of the statistical decay of metastable states, has derived a general expression for the rate of barrier crossing in a multidimensional system. By treating the N position coordinates, $\{q_i\}$ and their associated conjugate momenta $\{p_i\}$ as Gaussian random variables, he calculates a rate of decay of the metastable state that spans the intermediate to high friction regime. Moreover, the rate of variation of each Gaussian random variable is assumed to be different; as applied to polymer systems, each vertex has a nonidentical mass and friction constant. The approach we shall utilize is essentially an application of the method of Langer (although we do present two new contributions to the general theory in Sec. III and the Appendices). We focus explicitly on a particular model of polymer conformational transitions and consider in far greater detail the nature of the reaction coordinate in the vicinity of the saddle point. Finally, we note in passing that the general method should also be applicable to chemical reactions.

The paper is organized as follows: the molecular model is described in Sec. II. Then, in Secs. III–V, the steady state solution of the generalized Fokker–Planck equation is employed to determine the reaction coordinate in the vicinity of the saddle point, and to obtain an expression for k, the rate of conformational transition of a bond located in a heterogeneous chain molecule. Section VI presents an application of the method to six and 32 vertex chain molecules having nonidentical friction constants. The interplay of geometric and frictional effects on the reaction coordinate is clearly demonstrated. Finally, in Sec. VII, the major conclusions of this work are summarized, and possible future applications of the formalism are discussed.

II. MOLECULAR MODEL: THE FORM OF THE POTENTIAL

In order to apply the treatment to polymers, the specification of a molecular model is required. Consider a chain molecule in which both hydrodynamic and excluded volume interactions are entirely absent. These approximations should cause no serious qualitative difficulties on the time and distance scales relevant to conformational transitions. The potential is restricted to interactions along the backbone as is described below.

Let the molecule consist of $N-1$ bonds connecting N nonidentical vertices, labeled 0 to $N-1$. Figure 1 defines the bond fixed coordinate systems. For convenience, we assume that the molecule is linear, but with only a few minor modifications of notation the treatment is applicable to branched molecules. The mass and friction constant of the ith vertex are given by m_i and ζ_i, respectively.

The bond length of the ith bond b_i is maintained near a value $b_{0,i}$ by a potential, $V_{b,i}(b_i)$ that is quadratic in the bond length:

$$V_{b,i}(b_i) = \tfrac{1}{2}\gamma_{b,i}(b_i - b_{i,0})^2 , \tag{2.1}$$

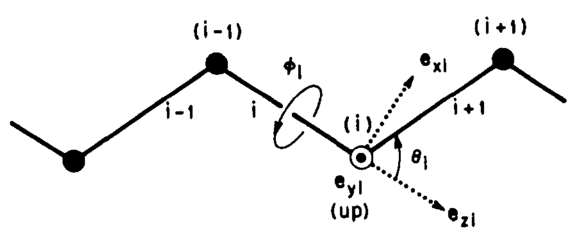

FIG. 1. The internal coordinate system used to specify the potential.

with $\gamma_{b,i}$ the bond stretching force constant of the ith bond. Furthermore, the bond angle θ_i, acute for tetrahedral bonds, is kept near a value $\theta_{0,i}$ by the potential

$$V_{\theta,i}(\theta) = \tfrac{1}{2}\gamma_{\theta,i}(\cos\theta_i - \cos\theta_{0,i})^2 \; . \tag{2.2}$$

Here, $\gamma_{\theta,i}$ is the angle bending force constant associated with the angle between bonds i and $i+1$. Moreover, bond rotation is characterized by the torsional angle ϕ_i, defined as the angle between the plane containing bonds $i-1$ and i and the plane containing bonds i and $i+1$. The torsional potential has been taken to be of the form

$$V_{\phi,i}(\phi_i) = \gamma_{\phi,i} \sum_{n=0}^{5} a_{n,i} \cos^n \phi_i \; . \tag{2.3}$$

We shall consider a potential in which the *trans* state $\phi_i = 0$ is the lowest in energy. A typical $V_{\phi,i}(\phi_i)$ is depicted in Fig. 2.

In our subsequent treatment, the behavior of $V_{\phi,i}(\phi_i)$ in the vicinity of its minima and maxima will be needed. Consequently, let

$$V_{\phi,i}(\phi_i) = \tfrac{1}{2}\gamma_{t,i}\phi_i^2 \; , \quad \text{near } trans \; , \tag{2.4}$$

$$V_{\phi,i}(\phi_i) = E_{g,i} + \tfrac{1}{2}\gamma_{g,i}(\phi_i \pm \phi_{g,i})^2 \; , \quad \text{near } gauche \; , \tag{2.5}$$

$$V_{\phi,i}(\phi_i) = E_i^* - \tfrac{1}{2}\gamma_i^*(\phi \pm \phi_i^*)^2 \; , \quad \text{near the } t-g \text{ barrier} \; . \tag{2.6}$$

The total potential is

$$V = \sum_{i=1}^{N-1} V_{b,i}(b_i) + \sum_{i=1}^{N-2} V_{\theta,i}(\theta_i) + \sum_{i=2}^{N-2} V_{\phi,i}(\phi_i) \; . \tag{2.7}$$

To proceed further, the behavior of the potential near the initial state well $r^0 = (x_1^0, x_2^0, \ldots x_{3N}^0)$ is needed. Let us write

$$V(\mathbf{r}) = \frac{1}{2} \sum_{i,j=1}^{3N} V_{ij}(x_i - x_i^0)(x_j - x_j^0) \; . \tag{2.8}$$

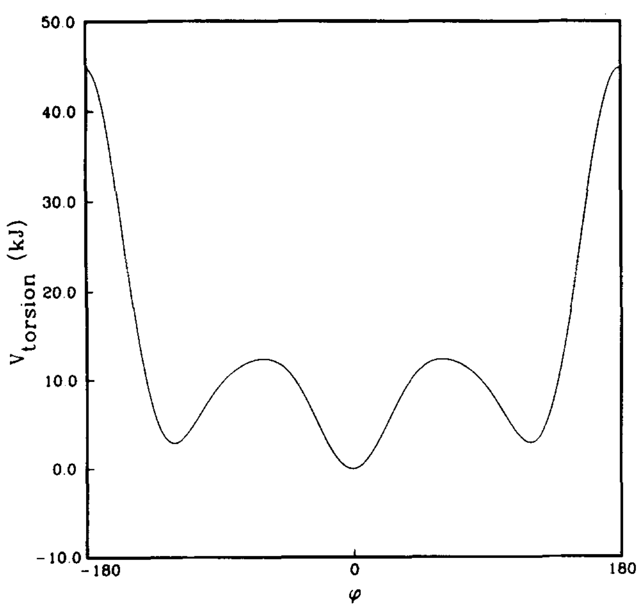

FIG. 2. A representative torsional potential $V_\phi(\phi)$ for rotational states in a chain molecule.

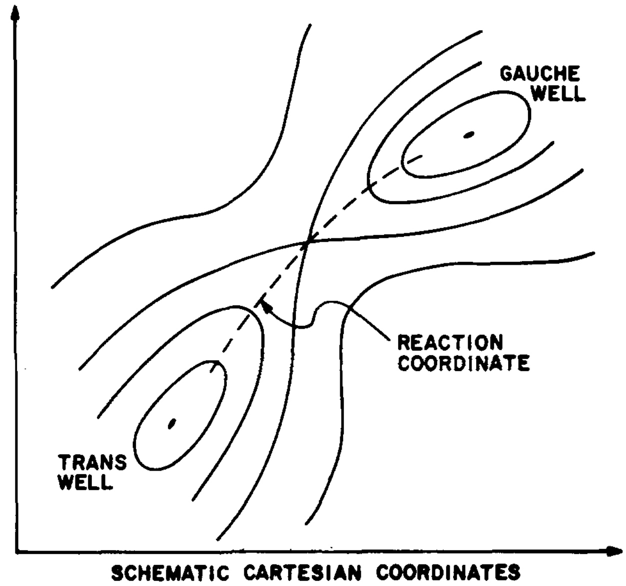

FIG. 3. A schematic representation of the potential in $3N$ dimensional space. Transitions occur from the *trans* to the *gauche* well by passing near the saddle point.

V is a symmetric non-negative definite matrix with six zero eigenvalues. It may be constructed from the Cartesian representation of Eq. (2.7). An explicit procedure for setting up the matrix may be found in Appendix A of Skolnick and Helfand.[1]

Near the saddle point $\mathbf{r}^* = (x_1^*, x_2^*, \ldots x_{3N}^*)$, the potential may be approximated by

$$V(r) = E_i^* + \tfrac{1}{2}\,\mathbf{q}\cdot\mathbf{W}\cdot\mathbf{q} \; , \tag{2.9}$$

$$q_j = x_j - x_j^* \; .$$

W is a symmetric $3N \times 3N$ matrix with *one* negative eigenvalue λ^*. The eigenvector corresponding to λ^*,

$$\mathbf{q}^* = (q_1^*, q_2^*, \ldots q_{3N}^*) \; ,$$

points in the direction of the path of steepest descent from the saddle point on the potential energy surface. For chain molecules composed of identical vertices, $\mathbf{q}^*$ also points in the direction of the reaction coordinate, a fact demonstrated in Sec. III. It is appropriate to note that in the development of the multidimensional reaction rate theory, it is the quadratic nature of Eqs. (2.8) and (2.9) that enables one to obtain a closed form solution. The relevant parameters for a polymethylene chain may be found in Refs. 1 or 7 (the parameters of the potential will not be taken as dependent on vertex index i). For other molecules, similar knowledge of the potential surface is necessary.

III. CONFORMATIONAL TRANSITION RATE FOR HETEROGENEOUS POLYMERS

Following Kramers,[22] we seek a solution to the Fokker–Planck equation corresponding to an average steady state flux over the barrier. The steady state is maintained by effectively withdrawing from the ensemble systems which have completed the transition, and restoring them far on the initial state side in an equilibrium distribution. A solution of this type may be constructed in terms of a product of an equilibrium distribution multiplied by a correction factor $g(u)$ where u is a single collective variable.

As stated in the introduction we calculate the rate by following Langer's version[26] of the generalization of Kramers' theory[22] to multivariable systems. Let us briefly outline that solution here, with some further details and extensions discussed in Appendices A–C. Although Langer presents his results in terms of $6N$ generalized coordinates, we will find it convenient at times to continue to distinguish between the position and momentum variables. At other times we will use the vector symbol η to represent all $6N$ variables, the first $3N$ components of which are denoted at $\mathbf{q} = (q_1, q_2, \ldots, q_{3N})$ and the remaining $3N$ as $\mathbf{p} = (p_1, p_2, \ldots, p_{3N})$. Thus, the Fokker–Planck equation may be written in the form of a continuity equation

$$\frac{\partial f(\eta)}{\partial t} = -\nabla_\eta \cdot \mathbf{J} , \tag{3.1}$$

where $\mathbf{J}$ is a probability current density in the $6N$-dimensional phase space. In a region where the energy is a quadratic form in the components of η, $\mathbf{J}$ is a linear operator acting on the distribution function f. In particular, near the saddle point,

$$J_j = \sum_{k=1}^{6N} \left[\sum_{l=1}^{6N} C_{jl} H_{lk} \eta_k + k_B T C_{jk} \frac{\partial}{\partial \eta_k} \right] f(\eta) , \tag{3.2}$$

$$\mathbf{C} = \begin{pmatrix} 0 & -1 \\ 1 & \zeta \end{pmatrix} , \tag{3.3}$$

$$\mathbf{H} = \begin{pmatrix} \mathbf{W} & 0 \\ 0 & \mathbf{M}^{-1} \end{pmatrix} . \tag{3.4}$$

The $6N$-dimensional matrices $\mathbf{C}$ and $\mathbf{H}$ have been written as blocks of $3N$ dimensional matrices. ζ and $\mathbf{M}$ are diagonal matrices with ii element equal to the friction constant and mass, respectively, of the vertex to which i refers. $\mathbf{H}$ is the matrix of the Hamiltonian quadratic form near the saddle point [cf. definition of $\mathbf{W}$ in Eq. (2.9)]; i.e.,

$$E \approx E^* + \frac{1}{2} \sum_{i,j=1}^{6N} H_{ij} \eta_i \eta_j . \tag{3.5}$$

Langer's next step is to convert to a basis such that $\mathbf{H}$ is diagonal, so that modes which do not affect the energy (modes corresponding to zero eigenvalues of $\mathbf{H}$), such as translations and rotations, can be separated out. In Appendix B, we show that this is not necessary. The advantage gained is a great simplification of the programming of the calculations, as well as the exposition of the theory.

A solution of the Fokker–Planck equation is sought which reduces to the equilibrium distribution far from the hypersurface dividing initial from final state and on the initial-state side. On the final-state side, the distribution function goes asymptotically to zero. As Kramers suggested, such a solution can be achieved by writing the distribution function as

$$f(\eta) = g(u) f_{\mathrm{eq}}(\eta) , \tag{3.6}$$

$$f_{\mathrm{eq}}(\eta) \approx \exp[-E(\eta)/k_B T]/Z_A . \tag{3.7}$$

Z_A is a partition function for states centered about the initial-state potential minimum. Its general form is discussed in Appendix D. As shown in Ref. 1, a simple form is appropriate for the potential of Sec. II. The function $g(u)$ in Eq. (3.6) depends only on a single variable which is a linear combination of the η variables:

$$u = \sum_{i=1}^{6N} U_i^* \eta_i , \tag{3.8}$$

$$= \sum_{i=1}^{3N} U_{qi}^* q_i + U_{pi}^* p_i . \tag{3.9}$$

When Eq. (3.8) is substituted into the Fokker–Planck equation, one finds that for g to be a function of a single variable $\mathbf{U}^*$ must satisfy the eigenvalue equation

$$\mathbf{HCU} = \kappa \mathbf{U} . \tag{3.10}$$

Due to the negative curvature of the potential energy surface in one direction moving by maximum descent from the saddle point and positive curvature in other directions, $\mathbf{H}$ has one negative eigenvalue which we call λ^*. $\mathbf{HC}$ has one negative eigenvalue, too. Henceforth, κ^* will stand for this eigenvalue and $\mathbf{U}^*$ will be the corresponding right eigenvector.

When u is defined as in the previous paragraph, the solution to the Fokker–Planck equation for g which goes to unity well on the initial-state side and to zero on the final-state side is

$$g(u) = \operatorname{erfc}\left[\left(\frac{|\kappa^*|}{2k_B T \hat{\zeta}}\right)^{1/2} u\right] , \tag{3.11}$$

$$\hat{\zeta} = \sum_{i=1}^{3N} \zeta_i (U_{pi}^*)^2 . \tag{3.12}$$

(erfc is the complementary error function).

The flux through a hyperplane passing through the saddle point and dividing initial from final state is the reaction rate k. Langer calculates this flux and finds

$$k = |\kappa^*| \left(\frac{k_B T}{2\pi |\lambda^*|}\right)^{1/2} \frac{Z^*}{Z_A} \exp\left(-\frac{E^*}{k_B T}\right) , \tag{3.13}$$

where Z_A was defined previously as a partition function associated with the initial state well and Z^* is a partition function associated with the reaction barrier for all degrees of freedom orthogonal to the one unstable mode of the potential at the saddle point (cf. Appendix D). When the potential can be written as a sum of potentials for independent modes the formula for k can be taken a step further than Langer's result, and a considerable simplification occurs.[1] This is the case for the model discussed in Sec. II where the potential was written as a sum of bond, bond angle, and torsional angle terms. The final result for the rate is

$$k = \frac{|\kappa^*|}{2\pi} \left(\frac{\gamma_t}{\gamma^*}\right)^{1/2} \exp\left(-\frac{E^*}{k_B T}\right) , \tag{3.14}$$

where κ^* is the negative eigenvalue in Eq. (3.10), γ_t and γ^* are force constants of the torsional potential for the transforming bond as defined in Eqs. (2.4) and (2.6), and E^* is the activation energy of this bond. Thus, the only part of the formula requiring computation is the determination of κ^*.

IV. THE REACTION COORDINATE

Equation (3.14) provides a means of calculating the rates of conformational transitions. Additionally, much physical insight is provided by knowledge of the motions of the various degrees of freedom along the reaction coordinate. When all friction constants are equal, the reaction coordinate is the path of steepest descent from the saddle point of the potential energy.[1] For the general case, Langer suggests that the reaction coordinate be identified in the following way. In the region near the saddle point, recall that the current, Eq. (3.2), can be written as a linear operator in the variables η_i acting on the probability distribution. Thus, the Fokker–Planck equation (3.1) may be multiplied by η and integrated over all space to obtain as an equation for $\langle\eta\rangle$

$$\frac{d\langle\eta\rangle}{dt} = -\mathbf{CH}\langle\eta\rangle \ . \tag{4.1}$$

It is easily shown that **CH** has the same set of eigenvalues as **HC**, and that the eigenvectors are **CU**.

In particular there is one mode of motion, associated with the negative eigenvalue κ^*, which satisfies

$$\langle\eta\rangle = \rho^* e^{-\kappa^* t} \ , \tag{4.2}$$

where

$$\mathbf{CH}\rho^* = \kappa^*\rho^* \ . \tag{4.3}$$

Since κ^* is negative, this deviation from the saddle point grows with time, and more rapidly than for any other deviation in phase space. Thus, ρ^* is to be identified as the reaction mode.

V. SPECIAL CASES

A. The high friction limit

Consider Eq. (4.3) for κ^* and ρ^*, which in block form may be written

$$\begin{pmatrix} 0 & -1 \\ 1 & \boldsymbol{\zeta} \end{pmatrix}\begin{pmatrix} \mathbf{W} & 0 \\ 0 & \mathbf{M}^{-1} \end{pmatrix}\begin{pmatrix} \rho_q^* \\ \rho_p^* \end{pmatrix} = \kappa^*\begin{pmatrix} \rho_q^* \\ \rho_p^* \end{pmatrix}, \tag{5.1}$$

or, multiplied out,

$$-\mathbf{M}^{-1}\rho_p^* = \kappa^*\rho_q^* \ , \tag{5.2}$$

$$\mathbf{W}\rho_q^* + \boldsymbol{\zeta}\mathbf{M}^{-1}\rho_p^* = \kappa^*\rho_q^* \ . \tag{5.3}$$

With ρ_p^* eliminated, this becomes

$$\mathbf{W}\rho_q^* = (\kappa^*\boldsymbol{\zeta} - \kappa^{*2}\mathbf{M})\rho_q^* \ . \tag{5.4}$$

In the limit of high friction, $\kappa^* = O(\zeta^{-1})$ in order to keep the right-hand side of the same order in $\boldsymbol{\zeta}$ as the left [the solution for which the right-hand side is $O(\zeta^2)$ does not have negative eigenvalues]. Details are given in Appendix C. Thus, the term $\kappa^{*2}\mathbf{M}$ becomes negligible and the eigenvalue equation reduces to

$$\mathbf{W}\rho_q^* = \kappa^*\boldsymbol{\zeta}\rho_q^* \ , \tag{5.5}$$

with the eigenvectors ρ_q^* corresponding to the negative eigenvalue being the reaction coordinate in position space.

A physical significance can be attached to Eq. (5.5) by associating it with a variational principle. Consider a small motion away from the saddle point

$$d\mathbf{q} = \rho_q ds \tag{5.6}$$

taking place in time dt. The dissipation associated with this motion is

$$\rho_q \cdot \boldsymbol{\zeta} \cdot \rho_q (ds/dt)^2 \ , \tag{5.7}$$

while the energy decrease is

$$\tfrac{1}{2}\rho_q \cdot \mathbf{W} \cdot \rho_q (ds)^2 \ . \tag{5.8}$$

Ask the question: for a fixed amount of dissipation what direction of motion produces the greatest energy decrease? The answer is ρ_q^* given by Eq. (5.5). In keeping with this derivation, we will normalize ρ_q^* so that

$$\rho_q^* \cdot \boldsymbol{\zeta} \cdot \rho_q^* = \text{constant} \ . \tag{5.9}$$

(With this normalization, κ^* and ρ_q^* could also be obtained variationally by minimizing $\rho_q^* \cdot \mathbf{W} \cdot \rho_q^*$.)

B. Low friction limit

In the low friction limit, the eigenvalue equation becomes

$$\mathbf{W}\rho_q^* = -\kappa^{*2}\mathbf{M}^{-1}\rho_q^* \ , \tag{5.10}$$

and κ^* must be selected as the negative square root of the resulting κ^{*2}.

C. General friction for identical vertices

In the case of identical vertices, $\boldsymbol{\zeta}$ and **M** are scalars, ζ and m times the unit matrix, respectively. The eigenvalue Eqs. (5.2)–(5.3) become

$$\mathbf{W}\rho_q^* = \lambda^*\rho_q^* \ , \tag{5.11}$$

$$m\kappa^{*2} - \zeta\kappa^* + \lambda^* = 0 \ , \tag{5.12}$$

where λ^* is the negative eigenvalue of **W**. The reaction coordinate is the corresponding eigenvector, i.e., the path of steepest descent from the saddle point. The transition rate is given by

$$k = \frac{|\lambda^*|}{2\pi\zeta}\left(\frac{\gamma_t}{\gamma^*}\right)^{1/2} \frac{1}{\left[\frac{1}{2} + \left(\frac{1}{4} + \frac{|\lambda^*|m}{\zeta^2}\right)^{1/2}\right]} \exp\left(-\frac{E^*}{k_B T}\right) \ , \tag{5.13}$$

$$= \frac{|\lambda^*|^{1/2}}{2\pi m^{1/2}}\left(\frac{\gamma_t}{\gamma^*}\right)^{1/2} \frac{1}{\left[\left(1 + \frac{\zeta^2}{4|\lambda^*|m}\right)^{1/2} + \frac{\zeta}{2(|\lambda^*|m)^{1/2}}\right]}$$

$$\times \exp\left(-\frac{E^*}{k_B T}\right) , \tag{5.14}$$

where the two forms are equivalent, but written in such a way as to bring out the high and low friction limits, respectively.

The criterion which governs whether one is in the high or low friction limit is $\zeta/(|\lambda^*|m)^{1/2}$ large or small, respectively. If the path of steepest descent is not delocalized to an unusually large extent then $|\lambda^*|$

$= O(\gamma^*)$. In the case of heterogeneous friction constants and masses, a typical ζ or m may be used in the criterion if there are not large differences in these parameters for the various centers. Otherwise, the full Eq. (5.4) must be studied.

VI. CALCULATIONS

To assess the effect exerted by nonidentical vertex friction constants a numerical study was performed of the rate of conformational transition rate k for a central bond $t-g$ transition in six and 32 vertex chains with various tail conformations. All masses were kept equal, but the odd and even numbered vertices (recall that the numbering system goes from 0 to $N-1$) were assigned different values for the friction constant: ζ_o and ζ_e. The mean value

$$\bar{\zeta} = \tfrac{1}{2}(\zeta_o + \zeta_e) \tag{6.1}$$

was maintained at 1.4×10^{-3} kg/s ($\hat{\beta} \equiv \bar{\zeta}/m = 10^5$ ns^{-1}), but the ratio ζ_o/ζ_e was assigned value of 1, 2, $\frac{1}{2}$, 6 and $\frac{1}{6}$. The potential and other parameters were those appropriate to polyethylene, as used previously.[1] The temperature was taken to be 372 K so that $E^*/k_BT = 4$. For these parameters, it was appropriate to employ the high friction limit equations (a few explicit comparisons with the general friction calculations confirmed that differences were small). The transition rates for a variety of conformations of the tails attached to the transforming bond are presented in Tables I and II.

To understand the manner in which the transition rates depend on the tails' conformations it is useful to examine the reaction coordinates. For the 32 vertex chains, these are fairly representative of the localized modes in long polymer. The nature of the transformation process becomes more transparent if the vertex displacements representing the reaction coordinate in Cartesian coordinates are transformed to the equivalent bond stretching, angle bending, and torsional motions. Consider a small displacement of the vertices of the polymer from the saddle point of a transition along the reaction coordinate such that vertex i moves $\rho_i^* ds$ (three-dimensional vectors) with normalization

$$\sum_{i=0}^{N-1} \zeta_i |\rho_i^*|^2 = \bar{\zeta} \tag{6.2}$$

TABLE I. Rate of central bond $t\to g^+$ transition in a six vertex chain for various tail conformations.[a]

Initial state conformation	Rate for ζ_o/ζ_e				
	1	2	1/2	6	1/6
ttt	16.05	16.66	16.66	19.75	19.75
ttg^+	12.56	13.57	12.92	15.74	19.15
ttg^-	10.81	10.35	12.07	15.74	10.81
g^+tg^+	5.87	6.34	6.34	9.58	9.58
g^-tg^+	5.04	5.67	5.09	6.30	8.80
g^-tg^-	4.36	4.61	4.61	6.02	6.02

[a] $(\zeta_0+\zeta_e)/2m = \hat{\beta} = 1\times10^5$ ns^{-1}, $E^*/k_BT = 4$.

TABLE II. Rate of central bond $t\to g^+$ transition in a 32 vertex chain for various tail conformation.[a]

Initial state conformation[b]	Rate for ζ_0/ζ_e				
	1	2	1/2	6	1/6
$(\ldots ttt)t(ttt\ldots)$	4.28	4.50	4.50	5.80	5.80
$(\ldots ttt)t(g^+tt\ldots)$	3.07	3.07	3.52	3.84	5.64
$(\ldots ttt)t(g^-tt\ldots)$	2.20	2.44	2.20	3.36	2.60
$(\ldots ttg^+)t(g^+tt\ldots)$	0.419	0.421	0.421	0.434	0.434
$(\ldots ttg^-)t(g^+tt\ldots)$	0.177	0.176	0.178	0.177	0.181
$(\ldots ttg^-)t(g^-tt\ldots)$	0.110	0.110	0.110	0.110	0.110
$(\ldots ttt)t(tg^+t\ldots)$	5.86	6.11	6.13	7.51	7.52
$(\ldots ttt)t(tg^-t\ldots)$	4.21	4.45	4.30	5.50	5.06
$(\ldots tg^+t)t(tg^+t\ldots)$	6.13	6.33	6.33	7.30	7.30
$(\ldots tg^-t)t(tg^+t\ldots)$	5.08	5.14	5.31	5.71	6.14
$(\ldots tg^-t)t(tg^-t\ldots)$	4.43	4.53	4.53	5.04	5.04
$(\ldots ttt)t(ttg^+\ldots)$	2.89	3.06	3.02	3.98	3.85
$(\ldots ttt)t(ttg^-\ldots)$	2.97	3.17	3.06	4.11	3.74
$(\ldots g^+tt)t(ttg^+\ldots)$	0.861	0.873	0.873	0.927	0.927
$(\ldots g^-tt)t(ttg^+\ldots)$	0.889	0.890	0.906	0.915	0.958
$(\ldots g^-tt)t(ttg^-\ldots)$	0.985	0.994	0.994	1.03	1.03

[a] $(\zeta_0+\zeta_e)/2m = \hat{\beta} = 1\times10^5$ ns^{-1}, $E^*/k_BT = 4$.

[b] The conformational sequences denoted by ... are all *trans*.

(the $3N$-dimensional vector ρ^* was called ρ_q^* in earlier sections). The change in the ith torsional angle associated with this motion is

$$d\phi_i = D_{\phi i}\, ds \ . \tag{6.3}$$

Likewise, the ith bond vector changes length by

$$db_i = D_{bi}\, ds \tag{6.4}$$

and the ith bond angle by

$$d\theta_i = D_{\theta i}\, ds \ . \tag{6.5}$$

Explicit expressions for $D_{\phi i}$, D_{bi}, and $D_{\theta i}$ in terms of ρ^* have been given in Appendix C of Ref. 1, and representative values reported for transformations of chains with all friction constants equal. An effort was made to relate, descriptively, the geometric aspects of the tails to the transition rate.

Several general principles govern this qualitative linkage of rate to conformation. One is that the reaction coordinate must be a localized mode,[1,2] so as to minimize the frictional resistance to motions associated with descent in energy from the saddle point. Localization can be achieved by distortion of neighboring degrees of freedom accompanying the rotation of the central bond. For these distortions not to involve a large increase of energy, they utilize, primarily, torsions of other bonds, the softest degrees of freedom. A particularly effective means of localizing any motion which involves rotation about some axis is to have counter-rotation about parallel, or near parallel, bonds (or rotation in the same sense about antiparallel

TABLE III. Localized mode for central (16th) bond $t \rightarrow g^+$ transition with initial state $(\ldots ttt)t(ttt\ldots)$, for a 32 vertex chain.

$\zeta_0/\zeta_e =$	1	6	1	6	1	6	1	6
i	$b_0 \lvert \rho_i^* \rvert \times 10^2$	$b_0 \lvert \rho_i^* \rvert \times 10^2$	$D_{\phi i}$	$D_{\phi i}$	$D_{\theta i}$	$D_{\theta i}$	$D_{bi} \times 10^2$	$D_{bi} \times 10^2$
10	3.29	6.32	−0.06	−0.06	−0.011	−0.013	0.58	0.85
11	1.14	1.50	−0.06	−0.05	−0.019	−0.025	0.53	0.65
12	4.53	7.94	−0.15	−0.15	−0.005	−0.010	0.98	1.55
13	1.80	1.34	0.02	0.09	−0.061	−0.085	0.66	0.85
14	3.60	6.41	−0.32	−0.35	0.048	0.066	1.53	2.36
15	7.41	7.13	0.17	0.31	−0.128	−0.177	1.07	1.31
16	7.41	9.51	1.54	1.80	−0.128	−0.150	1.82	2.18
17	3.60	2.67	0.17	0.15	0.048	0.050	1.07	0.91
18	1.80	4.14	−0.32	−0.34	−0.061	−0.055	1.53	1.37
19	4.53	2.99	0.02	−0.02	−0.005	−0.003	0.66	0.53
20	1.14	3.21	0.15	−0.14	−0.019	−0.011	0.98	0.73
21	3.29	1.74	−0.06	−0.07	−0.011	−0.015	0.53	0.49
i	ρ_{ix}^*	ρ_{ix}^*	ρ_{iy}^*	ρ_{iy}^*	ρ_{iz}^*	ρ_{iz}^*		
10	0.102	0.201	0.183	0.357	0.047	0.053		
11	−0.019	0.025	−0.021	0.055	0.069	0.077		
12	0.136	0.252	0.251	0.445	0.079	0.093		
13	−0.044	0.017	−0.077	0.015	0.078	0.085		
14	0.159	0.285	0.146	0.287	0.093	0.108		
15	−0.139	−0.069	−0.464	−0.459	−0.009	−0.040		
16	0.139	0.264	−0.464	−0.562	0.009	−0.019		
17	−0.159	−0.085	0.146	0.117	−0.093	−0.098		
18	0.044	0.147	−0.077	−0.211	−0.078	−0.084		
19	−0.136	−0.073	0.251	0.169	−0.079	−0.065		
20	0.019	0.106	−0.021	−0.172	−0.069	−0.058		
21	−0.102	−0.052	0.183	0.096	−0.047	−0.032		

bonds).[2,7] As a major example of this, when the transforming bond has a first neighbor bond which is *trans*, the second neighbor bond is parallel. The $t - g^+$ transition involves a positive rotation, so the parallel, second-neighbor bond would be expected to undergo a negative rotation.

By way of explicit illustration, consider a 32 vertex chain, with central bond, numbered 16, going from vertex 15 to 16. The reaction coordinate for a $t - g^+$ transition of bond 16, when all other bonds are *trans*, is given in Table III. The counter-rotations of bonds 14 and 18 are prominent.

Some interesting observations can be made, also, about the Cartesian components of the reaction coordinate. As illustrated in Fig. 4, place the molecule so that the central (16th) bond points in the $\mathbf{e}_z$ direction. Define the $\mathbf{e}_y$ direction as bisecting the actue angle between the plane of bonds 15 and 16 and the plane of bonds 16 and 17. Thus, if $\mathbf{b}_i$ is a vector along bond i defined by

$$\mathbf{b}_i = \mathbf{r}_i - \mathbf{r}_{i-1} , \tag{6.6}$$

then the y axis has unit vector

$$\mathbf{e}_y = (\mathbf{b}_{17} - \mathbf{b}_{15}) / \lvert \mathbf{b}_{17} - \mathbf{b}_{15} \rvert . \tag{6.7}$$

The vector $\mathbf{e}_x$ completes a right-hand coordinate system. As bond 16 rotates in a positive direction, the vertices of the right-hand tail move in the positive y direction and negative x direction. To counteract this motion, vertex 16, to which they are all attached, moves in the opposite sense. Note the prominent negative y component of ρ_{16}^* and the moderate positive x component. The tail motion, especially of even vertices, is also counteracted by a positive rotation of bond 17, which is observed. The effects on the left tail can be deduced from the fact that $\mathbf{e}_y$ is a C_2 axis (although this rotation reverses the sense of the defined bond directions).

To achieve an understanding of the effect of varying the friction constant on alternate vertices, it is first necessary to examine the relative magnitude of motion

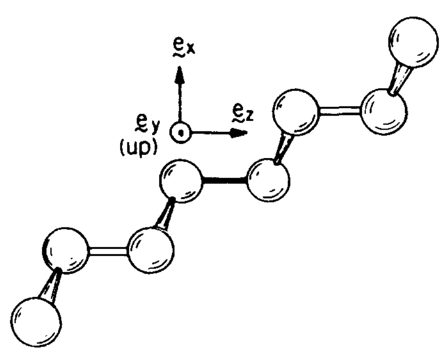

FIG. 4. Cartesian coordinate system, used for the reaction coordinate, centered on the transforming bond at the saddle state.

TABLE IV. Localized mode for central (16th) bond $t \rightarrow g^+$ transition with initial state $(\ldots ttt)t(g^+tt\ldots)$, for a 32 vertex chain.

$\zeta_0/\zeta_e =$	1	6	1/6	1	6	1/6
i	$b_0 \vert \rho_i^* \vert \times 10^2$	$b_0 \vert \rho_i^* \vert \times 10^2$	$b_0 \vert \rho_i^* \vert \times 10^2$	$D_{\phi i}$	$D_{\phi i}$	$D_{\phi i}$
10	4.21	8.29	2.02	−0.08	−0.08	−0.10
11	1.87	0.78	6.82	−0.06	−0.04	−0.11
12	5.06	9.31	3.01	−0.16	−0.16	−0.19
13	3.47	1.34	8.65	−0.01	0.06	−0.09
14	3.88	7.27	2.83	−0.29	−0.31	−0.35
15	9.07	7.66	10.43	0.06	0.17	0.01
16	3.41	2.63	3.65	1.23	1.34	1.65
17	2.81	2.31	5.62	−0.11	−0.11	−0.19
18	0.95	0.98	1.44	0.18	0.18	0.24
19	3.21	2.43	5.93	−0.04	−0.03	−0.05
20	1.17	0.87	1.23	0.07	0.05	0.09
21	2.24	1.33	4.41	0.02	0.02	0.05

of various vertices for $\zeta_o = \zeta_e$ as given the column labeled $b_0|\rho_i|$ in Table III. In the left tail, there is a large motion in the even vertices 14, 12, and 10, counteracted by a large opposite motion of vertex 15 which provides the twist of bond 16. Symmetrically, the right tail has a large motion in odd vertices 17, 19, and 21, countered by a large opposite motion of vertex 16. When the ratio of friction constants is made $\zeta_o/\zeta_e = 6$ the rate increases by 36%. The motion of the even vertices in the left tail becomes even more prominent, and the motion of vertex 15 is only moderately suppressed. In the right tail, the even vertices contribute to a much greater extent and a large motion of vertex 16 adds to the twist. Examination of the internal coordinates D_ϕ, D_θ, and D_b reveals that there is a small net shift of the motion to the left tail.

Another observation is that the greater negative y motion of vertex 16 compared with 15 amounts to a positive rotation of this bond about the $\mathbf{e}_x$ axis. Such a motion is counteracted by counter-rotations about parallel bonds such as 15 and 17. Note that this shows up especially in $D_{\phi 15}$. The positive rotation of bond 15 is also of great importance in counteracting motion of the immobile vertex 13.

When bond 17 is made g^+ bond 18 is not parallel to 16 so that counter-rotation of 18 is not an effective means of localizing motion of the right tail. In fact, bond 18 can be thought of as being more nearly antiparallel to 16 so that some degree of tail localization is achieved by having $D_{\phi 18}$ positive. However, the main feature of the reaction coordinate (Table IV) is that it concentrates motion in the left and uses a large countermotion of vertex 15 (larger than all *trans*) to counteract that motion. When $\zeta_o/\zeta_e = 6$ that countermotion of vertex 15 is inhibited and the rate goes up by only 25%. When $\zeta_o/\zeta_e = 1/6$, the combination of increased mobility of vertex 15 and more mobility in the right tail makes the rate go up by 84% relative to $\zeta_o/\zeta_e = 1$.

When bond 17 is g^- the right tail is even more incapable of localizing the motion via torsional distortions and the rate is lower than for bond 17 being g^+. However, not as great a motion of vertex 15 is needed to counteract the left tail's distortions (cf. Table V). The left tail's motions are greater in the even vertices, as

TABLE V. Localized mode for central (16th) bond $t \rightarrow g^+$ transition with initial state $(\ldots ttt)t(g^-tt\ldots)$, for a 32 vertex chain.

$\zeta_0/\zeta_e =$	1	6	1/6	1	6	1/6
i	$b_0 \vert \rho_i^* \vert \times 10^2$	$b_0 \vert \rho_i^* \vert \times 10^2$	$b_0 \vert \rho_i^* \vert \times 10^2$	$D_{\phi i}$	$D_{\phi i}$	$D_{\phi i}$
10	4.66	8.60	2.82	−0.066	−0.068	−0.050
11	1.41	1.21	4.54	−0.042	−0.033	−0.050
12	5.60	9.73	3.93	−0.136	−0.148	−0.121
13	2.37	1.17	5.25	0.016	0.072	0.003
14	4.52	7.80	3.47	−0.259	−0.303	−0.264
15	7.31	6.92	9.77	0.115	0.219	0.126
16	3.91	3.90	4.36	1.162	1.391	1.307
17	1.65	1.82	1.95	0.008	−0.003	0.043
18	3.09	2.74	3.79	−0.004	0.004	−0.024
19	3.33	2.85	3.92	−0.005	−0.014	0.018
20	2.88	2.39	3.20	0.005	0.011	−0.002
21	2.26	1.66	2.49	−0.008	−0.010	−0.001

usual, but not as great a motion of odd vertex 15 is needed to counteract it. The result is that the rate is now higher for $\zeta_o/\zeta_e = 6$ than for $\zeta_o/\zeta_e = 1/6$ (opposite to the case where bond 17 was g^+).

From the above discussion, one can gather that the effect of the change of mobility of a certain set of vertices is not always easily assessed intuitively. This is because there are generally competing effects and one cannot easily tell which will dominate. In particular, for a transition of bond 16, motion on the right concentrates on the even vertex 16; but in the tail it concentrates on odd vertices 17, 19, 21,... (similarly on the left motion concentrates on 15, 14, 12, 10,...). This difficulty is to be contrasted with the earlier study of how tail conformation affected rates, where general principles were more easily extracted.[1]

VII. OBSERVATIONS AND DISCUSSION

In the context of a single independent transition event theory, a general expression for the rate of conformation transition k of a bond in a heterogeneous polymer molecule has been derived and is applicable from the moderately low to high friction limit. The rate expression can be greatly simplified if the backbone potential can be decomposed into independent angle bending, bond stretching, and torsional angle contributions. Then, k depends on the ratio of the torsional force constants, the barrier height of the rotational angle undergoing the transition, and on the eigenvalue of a specified matrix. In the presence of nonidentical vertex friction constants, the negative eigenvalue's eigenvector of the potential matrix and the reaction coordinate are oriented in different directions. This occurs because the reaction coordinate reflects the role of frictional as well as geometric rigidity in the creation of the localized mode responsible for conformational transitions. Ample demonstrations of these effects are seen on application of the theory to six and 32 vertex chains composed of vertices of alternating mobilities.

We note that the current treatment is also applicable to polymers having a nondiagonal friction matrix.

In future work, we plan to calculate rates of transition in polystyrenelike molecules; the effect of nonidentical friction constants and masses will be systematically examined. It is hoped that qualitative guidance on the level of molecular detail necessary to treat conformational transitions in heterogeneous polymers will emerge.

Additional Brownian and molecular dynamics simulations on heterogeneous polymers, and simulations that span the intermediate to high friction regimes, are called for. Such work should provide insight into the range of applicability of the model presented here.

APPENDIX A: NOTATIONAL DIFFERENCES FROM LANGER'S THEORY

In the development of Sec. III, we have followed Langer's development rather closely. The reader interested in further mathematical detail should return to Langer's fine exposition.[26] There are two extensions we have made to the theory. Because these have wide applicability, we discuss them in greater detail in Appendices B and C.

Regrettably, we have found it necessary to make a few notational changes so as not to have conflicts in notation. The matrix we call **C** is call M by Langer (our **M** matrix is the masses). Langer introduces the matrix Γ which for the present problem is given by

$$\boldsymbol{\Gamma} = k_B T \begin{pmatrix} \mathbf{0} & \mathbf{0} \\ 0 & \zeta \end{pmatrix} \tag{A1}$$

and

$$\mathbf{A} = \begin{pmatrix} 0 & 1 \\ -1 & \mathbf{0} \end{pmatrix} , \tag{A2}$$

so that our **C** (his M) is

$$\mathbf{C} = (\boldsymbol{\Gamma}/k_B T) - \mathbf{A} . \tag{A3}$$

Langer introduces the matrix **H** only in its diagonal form, with diagonal elements λ_i. Finally, our η_i are measured from the saddle point so Langer's $\bar{\eta}_i = 0$.

APPENDIX B: NEED THE NULL SPACE OF H BE EXPLICITLY REMOVED?

There are well known difficulties in this, and a variety of related problems, associated with zero eigenmodes of **H** corresponding to redundant variables such as overall translation and rotation. Langer chooses to avoid that difficulty by working in a basis for which **H** is diagonal, and explicitly omitting those modes. There are two minor inconveniences associated with this procedure. Firstly, it means that one must introduce additional notations referring to this basis. More serious is the fact that in practical calculations one feels compelled to carry out the prescribed procedure in the computer program, a task comparable in programming and running time to the other steps. We will now demonstrate that in reality the zero eigenmodes of **H** cause no difficulty, so that one may work in a natural geometric basis, such as the Cartesian positions and momenta.

Mathematically stated, Langer suggests the following procedure: Let $s_{i\alpha}$ be the ith element of the eigenvector of **H** corresponding to eigenvalue λ_α; i.e., **H** is diagonalized by an orthogonal transformation with the matrix **S** whose elements are $s_{i\alpha}$,

$$\sum_{ij} s_{i\alpha} H_{ij} s_{j\beta} = \lambda_\alpha \delta_{\alpha\beta} . \tag{B1}$$

Here α and β cover the values 1 to $6N$. However, one can divide the set of α into indices labeling the range R of **H** (space spanned by the eigenvectors corresponding to nonzero eigenvalues) and indices labeling the null space N. One can also consider a rectangular matrix S', with elements $s_{i\alpha}$, where i runs over all values, but α runs only over the range. Langer's procedure is essentially to transform all vectors and matrices with this rectangular matrix. Thus, one takes Eq. (3.10)

$$\sum_{kl} H_{ik} C_{kl} U_{l\beta} = U_{i\beta} \kappa_\beta , \quad \beta \in R \tag{B2}$$

and transforms it to [equivalent to Langer's Eq. (3.14)]

$$\sum_{\gamma}{}' \lambda_\alpha \tilde{C}_{\alpha\gamma} \tilde{U}_{\gamma\beta} = \tilde{U}_{\alpha\beta} \kappa_\beta , \quad \alpha, \beta \in R , \tag{B3}$$

where the prime on the summation indicates that $\gamma \in R$ and

$$\tilde{C}_{\alpha\gamma} = \sum_{ij} s_{i\alpha} C_{ij} s_{j\gamma} , \quad \alpha, \gamma \in R , \tag{B4}$$

$$\tilde{U}_{\alpha\beta} = \sum_{i} s_{i\alpha} U_{i\beta} , \quad \alpha, \beta \in R . \tag{B5}$$

Then he writes the variable u [cf. Eq. (3.8)] as

$$u = \sum_{\alpha} \tilde{U}_\alpha^* \xi_\alpha , \tag{B6}$$

$$\xi_\alpha = \sum_{i} s_{i\alpha} \eta_i , \quad \alpha \in R ; \tag{B7}$$

where $\tilde{U}_\alpha^* = \tilde{U}_{\alpha\beta}$ with β corresponding to the negative eigenvalue. U_i^*, introduced in Eq. (3.8), is given by

$$U_i^* = \sum_{\alpha}{}' s_{i\alpha} \tilde{U}_\alpha^* . \tag{B8}$$

Let us note that $s_{i\alpha}$, for $\alpha \in N$, are left eigenvectors of HC corresponding to eigenvalues zero. Right eigenvectors are orthogonal to left eigenvectors corresponding to different eigenvalues. Thus,

$$\tilde{U}_{\alpha\beta} \equiv \sum_{i} s_{i\alpha} U_{i\beta} = 0 , \quad \alpha \in N, \ \beta \in R . \tag{B9}$$

Therefore, even if the sum in Eq. (B6) defining u were extended to all α, the value of u would not change. Likewise, the eigenvalue Eq. (B3) can have the γ summation extended to all γ. As far as the physical quantities κ and $U_{i\alpha}$ are concerned, one gets the same results if one transforms with $\mathbf{S}'$ or $\mathbf{S}$, or if one does not transform variables at all.

Note however that the reaction coordinate ρ^*, given as an eigenvector of CH, is not orthogonal to the null space of H, i.e., orthogonal to translation and rotation. It is customary to define normal modes as not orthogonal to the null space, as in the case of molecules of unequal mass.[27] If the transformation with $\mathbf{S}'$ had been applied to CH, then ρ^* would have been orthogonal to the null space. ρ^* is used only to enhance intuition and not in calculations, so there is no physical effect of following one procedure or the other.

APPENDIX C: HIGH FRICTION LIMIT

We provide here further detail of the high friction limit discussed in Sec. V. The crucial observation there is that in the high friction limit $\kappa = O(\zeta^{-1})$. Using this observation in the rate equation (3.13), one obtains the well-known high friction result $k \sim \zeta^{-1}$. Examination of Eq. (5.2) reveals that $\rho_p = O(\zeta^{-1})$ if ρ_q is taken to be of $O(1)$. Thus, these modes are, in the limit, motions in space, one example being the reaction coordinate. They are $3N$ in number.

One may also consider modes for which $\kappa = O(\zeta)$. In the high friction limit, for the present problem, these are the very rapidly relaxing momentum modes. In the limit the eigenvalue equation, best seen from Eq. (5.3), is

$$\boldsymbol{\zeta} \mathbf{M}^{-1} \boldsymbol{\rho}_p = \kappa \boldsymbol{\rho}_p . \tag{C1}$$

When $\boldsymbol{\zeta}$ and $\mathbf{M}$ are diagonal the jth eigenvector has

$$\rho_{p,ij} = \delta_{ij} , \tag{C2}$$

with eigenvalue $\kappa_j = \zeta_j / m_j$. The $\boldsymbol{\rho}_q$ components are of $O(\zeta^{-1})$.

Langer has discussed a high friction limit in his paper. In his limit, the diagonal elements of $\boldsymbol{\Gamma}$ [cf. Eq. (A1)] are large. However, for the problem at hand, the spatial part of $\boldsymbol{\Gamma}$ is identically zero so that our spatial relaxation $\kappa = O(\zeta^{-1})$ modes are not obtained by him, and only $\kappa = O(\zeta)$ modes are found.

APPENDIX D: THE PARTITION FUNCTIONS

In Ref. 1, an extensive discussion is presented of the partition functions involved in the rate formula Eq. (3.13). In this appendix, we shall summarize those arguments and provide a guide to them.

The partition function Z_A could be an evaluation by the standard technique for a polyatomic molecule, as given, e.g., in Münster.[28] The partition function then involves the moment of inertia tensor and the eigenfrequencies of normal modes. On the other hand, when the energy is a sum of potentials for independent modes, it is far easier and more useful to proceed as follows. Start at one end of the chain and integrate over one vertex's coordinates relative to the fixed chain, using b_{i-1}, θ_{i-2}, and ϕ_{i-2}. Proceed down the chain integrating over the succeeding vertices. The result is a partition function which is a product of factors related to the individual degrees of freedom involved in the potential Eq. (2.7).

Before proceeding in like manner with the partition function Z^*, one must deal with the fact that the unstable mode has been eliminated. Formally one can restore that mode by multiplying and dividing by the unstable (negative frequency). However, the result is not a true partition function since the integral over space, in harmonic approximation for the potential, diverges. It is shown in Appendix B of Ref. 1 that one can modify the potential for the one unstable degree of freedom (torsion of the reacting bond) to make it stable, and obtain the result appropriate to the unstable potential by analytic continuation. In the resulting partition function, the integral over every degree of freedom is identical with that in Z_A, except for the integral over the ϕ of the transforming bond. It is in this way that one shows that

$$\left(\frac{2\pi k_B T}{|\lambda^*|}\right)^{1/2} \frac{Z^*}{Z_A} = \left(\frac{\gamma_t}{\gamma^*}\right)^{1/2} ,$$

the result needed to simplify Eqs. (3.13)–(3.14).

[1]J. Skolnick and E. Helfand, J. Chem. Phys. 72, 5489 (1980).
[2]E. Helfand, J. Chem. Phys. 54, 4651 (1971).
[3]J. H. Weiner and M. R. Pear, Macromolecules 10, 317 (1977).
[4]M. Fixman and G. T. Evans, J. Chem. Phys. 68, 195 (1978).
[5]E. Helfand, J. Chem. Phys. 68, 1010 (1978).
[6]E. Helfand, Z. R. Wasserman, and T. A. Weber, J. Chem.

Phys. **70**, 2016 (1979).
[7]E. Helfand, Z. R. Wasserman, and T. A. Weber, Macromolecules **13**, 526 (1980).
[8]R. S. Adler and K. F. Freed, J. Chem. Phys. **72**, 2032 (1980).
[9]B. Baysal, A. Lowry, H. Yu, and W. H. Stockmayer, in *Dielectric Properties of Polymers*, edited by F. E. Karasz (Plenum, New York, 1972).
[10]A. A. Jones, K. Matsuo, K. F. Kuhlman, F. Geny, and W. H. Stockmayer, Polym. Preprints **16**, 578 (1975) and references cited therein.
[11]H. Morawetz, Acc. Chem. Res. **3**, 354 (1970).
[12]T. P. Liao and H. Morawetz, Macromolecules **13**, 1228 (1980).
[13]T. F. Schatzki, J. Polym. Sci. **57**, 496 (1962).
[14]L. Monnerie and F. Geny, J. Chim. Phys. **66**, 1691 (1969).
[15]J. C. Keck, Discuss. Faraday Soc. **33**, 173 (1962).
[16]C. Bennett, in *Algorithms for Chemical Computations*, edited by R. E. Christoffersen (ACS Symposium Series, Washington, D.C., 1977), Vol. 46.
[17]J. L. Skinner and P. G. Wolynes, J. Chem. Phys. **69**, 2143 (1978).
[18]S. H. Northrup and J. T. Hynes, J. Chem. Phys. **73**, 2700 (1980).
[19]R. F. Grote and J. T. Hynes, J. Chem. Phys. **73**, 2715 (1980).
[20]J. A. Montgomery, Jr., D. Chandler, and B. J. Berne, J. Chem. Phys. **70**, 4056 (1979).
[21]C. Blomberg, Physica A **86**, 49 (1977).
[22]H. A. Kramers, Physica **7**, 284 (1940).
[23]H. C. Brinkman, Physica **22**, 149 (1956).
[24]R. Landauer and J. A. Swanson, Phys. Rev. **121**, 1668 (1961).
[25]J. S. Langer, Phys. Rev. Lett. **21**, 973 (1968).
[26]J. S. Langer, Ann. Phys. (N.Y.) **54**, 258 (1969).
[27]H. Goldstein, *Classical Mechanics* (Addison-Wesley, Cambridge, 1959).
[28]A. Münster, *Statistical Thermophysics*, *Vol. I* (Springer, Berlin, 1969).